ChemPhysChem

Research Article
doi.org/10.1002/cphc.202400374

Chemistry Europe
European Chemical Societies Publishing

www.chemphyschem.org

Deuterium Isotope Effect in Single Molecule Photophysics and Photochemistry of Hypericin

Liangxuan Wang,[a, b] Quan Liu,[a] Andrea Buchwald,[a] Frank Wackenhut,[a, c] Marc Brecht,[a, c] Johannes Gierschner,*[a, b] and Alfred J. Meixner*[a]

The peripherical protons of the dye molecule hypericin can undergo structural interconversion (tautomerization) between different isomers separated by a low energy barrier with rates that depends sensitively on the interaction with local chemical environment defined by the nature of host material. We investigate the deuterium (D) isotope effect of hypericin tautomerism at the single-molecule level to avoid ensemble averaging in different polymer matrices by a combined spectroscopic and computational approach. In the 'innocent' PMMA matrix only *intra*molecular isotope effects on the internal conversion channel and tautomerization are observed; while PVA specifically interacts with the probe via H- and D-bonding. This establishes a single molecular picture on *intra*- and *inter*molecular nano-environment effects to control chromophore photophysics and -chemistry.

Introduction

Optical detection of single molecules in condensed matter has expanded far beyond the early low-temperature studies in crystals, to investigate single molecules in cells, in solution and in polymers. Detecting individual molecules optically gains the major advantage from avoiding ensemble averaging, providing direct access to inhomogeneous static or quasi-static distribution in nano-environments. As a consequence, it hence allows to observe kinetics, for instance, diffusion[1] and binding processes of nucleic acid[2] and proteins.[3] Especially, conformational dynamics are of interest, since they are difficult to observe or are hidden in a classical ensemble measurement.[4] Moreover, it allows access to spatial[5] as well as structural[6] information.[7]

Tautomerization is an *intra*molecular chemical reaction defined as structural interconversion of a molecule between two isomers separated by a low energy barrier, in which the position of a labile proton changes.[8] Particularly interesting is that the tautomerization rate in liquid solutions at room temperature is often on the order of MHz, but it can range over orders of magnitude depending on the temperature and the local environment. Embedding tautomerizable single molecules at low concentration in various polymer matrices at room temperature has unequivocally revealed that the rate in these molecules can vary dramatically reduced over time, such that tautomerization can be frozen for seconds and longer under ambient conditions.[4c]

Hypericin (Scheme 1), as a natural active ingredient in *Hypericum perforatum* (St. John's wort), has found tremendous interest in bio- and biomedical applications as photosensitizer, multifunctional agent in drugs due to its anti-depressive, anti-neoplastic, anti-tumor and anti-viral activity.[9] Furthermore, hypericin is not only of medical interest, but also a fascinating molecule for the investigation of fundamental physical and

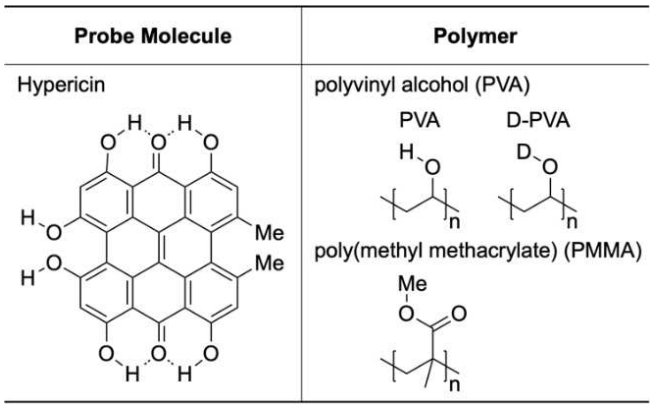

Scheme 1. Chemical structure of hypericin and the host polymers: PVA and PMMA.

[a] *L. Wang, Dr. Q. Liu, A. Buchwald, Dr. F. Wackenhut, Dr. M. Brecht, Dr. J. Gierschner, Prof. Dr. A. J. Meixner*
Institute of Physical and Theoretical Chemistry
Eberhard Karls Universität Tübingen
Auf der Morgenstelle 18, Tübingen 72076, Germany
E-mail: johannes.gierschner@imdea.org
alfred.meixner@uni-tuebingen.de

[b] *L. Wang, Dr. J. Gierschner*
Madrid Institute for Advanced Studies
IMDEA Nanoscience
Ciudad Universitaria de Cantoblanco, C/Faraday 9, Madrid 28049, Spain

[c] *Dr. F. Wackenhut, Dr. M. Brecht*
Center for Process Analysis and Technology (PA&T), School of Life Sciences and
Reutlingen Research Institute (RRI)
Reutlingen University
Alteburgstraße 150, Reutlingen 72762, Germany

Supporting information for this article is available on the WWW under https://doi.org/10.1002/cphc.202400374

chemical processes, as it can undergo de-/protonation, conformational transitions and tautomerization.[10] Proton migration around the perimeter of hypericin gives rise to ten tautomeric isomers.[10c,11] Direct observation of the tautomerization of hypericin in the polymer matrix was achieved in preliminary studies using confocal microscopy combined with an azimuthally polarized or radially polarized doughnut mode (APDM/RPDM) laser beam.[11] The tautomerization in hypericin occurs at the 'outer' part of the molecule and is hence very sensitive to the interaction of the chromophore with the host molecules. By altering the local optical and chemical nano-environment, one can modulate the radiative as well as non-radiative rates.[11–12] The modification of the local photonic environment can be achieved independently by enclosing the molecule between the two mirrors of a $\lambda/2$ Fabry-Pérot microcavity and varying their distance.[12b] As a result, the spontaneous emission rate is modified by the Purcell effect and leads to a variation in fluorescence lifetime.[12b]

In this work, we focus on the local chemical environment as reflected by the dielectric constant, oxygen permeability and solvent and/or water content of the polymer; all these factors can strongly influence the excited-state lifetime, dark state dynamics and survival time (photo-bleaching) of the probes. Furthermore, the investigation is extended to deuterated environments; deuteration causes only minor structural change, but has a considerable impact on the non-radiative decay path.[13] Due to the low pK_a (1.8) at the bay hydroxyl groups,[10b,14] H/D exchange can be easily achieved in solution. In addition, fluorescence correlation spectroscopy (FCS)[15] is used to analyze temporal dynamics of hypericin tautomerization; this allows to study how the tautomerization rate is influenced by the matrix in which the molecule is embedded or by exchanging the tunneling proton with deuterium. Last but not least, the experiments are complemented by (time-dependent) density functional theory ((TD)DFT) calculations, in which hypericin was embedded in an explicit solid matrix through a cluster model; this allows to study the *inter*molecular interactions, that largely influence the curvature of potential energy surface, and may give indications for the tunneling effect.

Experimental Section

Confocal Microscope

All measurements were performed with a home-built confocal scanning microscope. The sample was excited by a pulsed laser ($\lambda = 530$ nm, pulse duration < 100 ps, 20 MHz, LDH–P-FA-530 L, PicoQuant, 3 μW in front of the objective), focused on the sample via a high numerical aperture (NA=1.46, 63×, Carl Zeiss) oil objective lens. Scanning images were obtained by fixing the sample with magnets on a piezo-stage (P-527.3CL, Physik Instrumente). The fluorescence signal from the excitation spot was collected by the same objective lens and sent to two avalanche photodiodes (APDs, SPCM-AQR-14, PerkinElmer) via a 50/50 beam splitter. The APDs were connected to a time-correlated single photon counting (TCSPC) module (HydraHarp 400, PicoQuant), synchronized with the transistor transistor logic (TTL) signal, generated by the pulsed laser; a TTL from the APD is recorded for each detected photon and saved as a time-tagged time-resolved (TTTR) file.[16] The presence of single hypericin molecules was confirmed by antibunching measurements. (see Figure S1 in SI)

Materials and Sample Preparation

Hypericin (Burg-Apotheke, Königstein) was dissolved in ethanol (Uvasol, Merck) or in methanol-d^4 (99% atom D, Sigma-Aldrich), respectively, for H/D exchange; in the following denoted as D-hypericin. Poly (vinyl alcohol) (PVA, Mowiol 40–88, Sigma-Aldrich) was either dissolved in triply distilled water or in deuterium oxide (99.9% atom D, Sigma-Aldrich) (2 wt. %) for a complete H/D exchange of the hydroxyl group; in the following denoted as D-PVA, respectively. Poly (methyl methacrylate), PMMA (in anisole, AR–P 631-679 e-beam resists for nanometer lithography)[17] is commercially available. H- and D-hypericin concentrations of 10^{-9} M were used for single-molecule experiments. To prevent photobleaching as far as possible, the sample solutions were stored in a dark refrigerator. The preparation of thin films was carried out by spin-coating (20 μL solution approx. 6000 rpm over a period of 20 seconds). All the measurements were conducted under a laminar nitrogen flow to minimize the impact of oxygen quenching.

Computational Methods

The electronic ground, excited and transition state optimizations on the full structure of the system were carried out by (TD)DFT calculations. In all cases, the B3LYP functional with the standard 6–31G(d) basis set with dispersion correction (D3) was applied, as defined in the Gaussian16 program package.[18] As the work focuses on the nano-environmental effect on single hypericin molecules, we propose a realistic model of the single hypericin molecule surrounded by an explicit polymer matrix, describing specific solvent-solute interactions at the electronic level. A full geometry optimization of hypericin in PVA/PMMA was carried out. (see Figure 1(e)) In detail, one hypericin molecule was surrounded by either seven PMMA or 14 PVA oligomers (with n=5 repeating units) within the Packmol package,[19] followed by 10 ns molecular dynamics (MD) simulations with Gromacs[20] adopting the GAFF force field, restraining the positions of the hypericin structure. All energy minima were confirmed by the absence of imaginary frequencies, whereas the transition states were characterized by one imaginary frequency with a proper mode, referring to a local maximum (a saddle point along the potential energy surface) and reflecting the dynamic pathway between two local maxima.[21] For the details of all calculations, see SI.

Results and Discussion

Hypericin is a dye molecule with a large π-electron system, whereby the methyl-substitutions at the *bay* region contribute to a distorted aromatic parent backbone (see Figure 1(d)). Besides, hypericin offers a rich structural variety of conformational and constitutional or structural isomers due to the presence of six hydroxyl and two keto groups, as well as naphthodianthrone core.[10b] Ensemble fluorescence lifetime measurements of H-hypericin in a PVA polymer matrix were described by us earlier,[22] giving an average lifetime of $\tau_F = 4.2 \pm 0.9$ ns and a quantum yield of $\Phi_F = 12.2\% \pm 1.2\%$. Such polymer matrices are commonly used in single molecule measurements to immobilize and photo-stabilize the

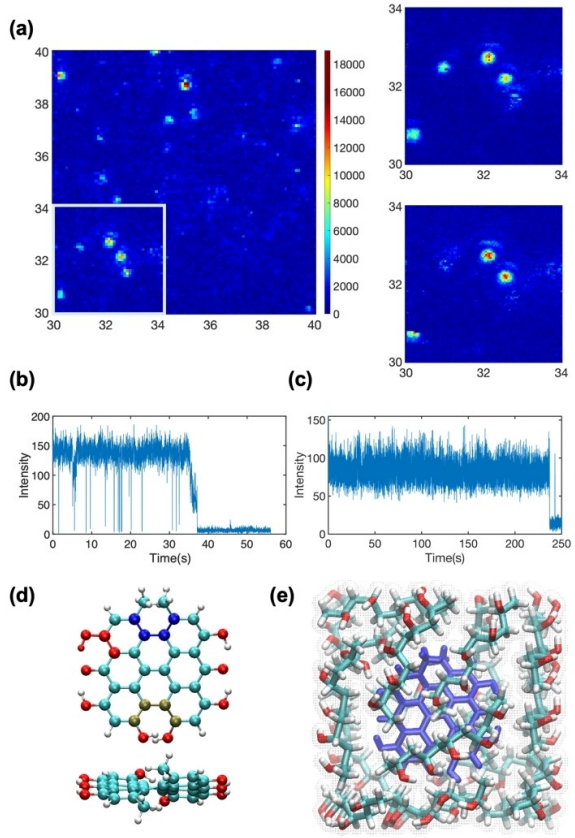

Figure 1. Fluorescence properties of single hypericin molecules. (a) Fluorescence images of single D-hypericin molecules embedded in D-PVA matrix. The inset is a close-up scan and shows a characteristic photobleaching event during the scanning process, scan unit in μm; (b) and (c) two explementary intensity time traces of single D-hypericin molecules in D-PVA and PMMA with a binning time of 10 ms; (d) chemical structure of hypericin with three dominating dihedral angles, blue: θ_{Me} (bay); green θ_{OH} (bay); and red: θ_{OH} (TS), for details see Table 2; (e) the cluster model of hypericin embedded in polymer matrix.

fluorophore.[23] In the current work, however, specific polymer-probe interactions are investigated. For this, we used PVA and PMMA, as both polymers are transparent with high light transmittance. The most pronounced feature of the PVA structure is the prevailing hydroxyl group (Scheme 1), which can form hydrogen (H/D) bonds with H- or D-hypericin, thus providing significant non-covalent interaction between the probe and the matrix. The deuterium isotope effect is expected to be observed in PVA as the D-bond is stronger compared to the H-bond due to the lower zero-point vibrational energy of the D-bond (*vide infra*).[24] PMMA, on the other hand, can be considered as an 'innocent' polymer host, as it does not provide functionalities which cause specific strong interactions; however it benefits from its high oxygen permeability.[25] Due to PVA's higher polarity, PVA exhibits a dielectric constant of 2.6,[26] while that of PMMA is 1.8.[17] Generally, matrices with a higher dielectric constant lead to a higher reaction field in response to the static electric dipole moment of an embedded molecule (for details, see Ref.[27] and literature cited therein).

Typical fluorescence images of single hypericin molecules at a 10×10 μm^2 scale, acquired by our home-built setup, are illustrated in Figure 1(a) on the left. The fluorescence images show isolated bright circular spots with a diffraction-limited diameter Gaussian-shaped intensity distribution; further details can be observed in the close-up views on the right side of Figure 1(a). Antibunching confirmed that single molecules with a minimal spatial distance of 1 μm, which is much larger that the diffraction limited focal spot of the confocal microscope, are observed; this is sufficient to detect only one molecule within the focal volume at a time. As discussed in former works,[11–12,22] variations in emissivity (or dynamical intensity fluctuation) can be attributed to (temporal) dark states of hypericin; the latter show populating kinetics resembling those of the triplet state or in other less- or non-emissive states.[28] In order to investigate the blinking dynamics of hypericin, single molecule intensity time traces were recorded. Two examples, namely D-hypericin in D-PVA (Figure 1(b)) and PMMA (Figure 1(c)) with a binning time of 10 ms were recorded until the dark state was reached and no further emission signal could be recorded after a duration of at least 20 s. The two exemplary intensity time traces show the characteristic "blinking" phenomenon consisting of discrete on-off (or bright-dark) transitions which agrees well with Figure 1(a). D-hypericin in D-PVA shows a higher intensity with stronger fluctuations during the 'on' periods. The fluctuations are magnitudes greater than the statistical noise, or instabilities of the excitation intensity as the off-state 40–55 s in Figure 1(b). This indicates on-off transitions on a much shorter timescale than seconds and are likely to be caused by intersystem crossing to a triplet state. In addition, shortly before the occurrence of persistent bleaching, there is often a sudden drop in intensities, indicating the tautomerization process. In stark contrast, D-hypericin in PMMA is rather stable not only in terms of fluctuation dynamics but also in terms of photostability. The decrease in on-off transition and longer survival time correspond qualitatively to the partial quenching due to the low oxygen exposure.

The influence of the local environments (PVA, PMMA) on the survival time and blinking dynamics (the on-off ratio) were analyzed statistically. The survival time is defined as the time before total photobleaching. Figure 2(a) and (b) illustrate the survival time for a single (D-)hypericin molecule in (D-)PVA and PMMA, respectively. At the first glace, we find the survival time in PMMA is much longer than that in PVA due to the low oxygen exposure. Applying an exponential fitting function on the data in Figure 2(a) and (b), we determine an average survival time of 28 s (22 s) for (D-)hypericin in (D-)PVA and 164 s (117 s) in PMMA. Deuteration contributes to a shorter survival time in the same polymer matrix.

The same fluorescence intensity time traces were used to study the blinking behavior by determining the on-off ratio, that is, the proportion of the 'on' period (bright state) to the total survival time ('on' and 'off' period). The 'on' period is defined as the fluorescence above the threshold (10% above the background intensity). An increased blinking corresponds to a decreased on-off ratio. Figure 2(c) and (d) presents the results of 'on' ratio for (D-)hypericin in PVA and PMMA. It can be clearly seen that (D-)hypericin in PMMA exhibits a significant amount of 'on' period with k_{on} close to 100%, reflecting a rather

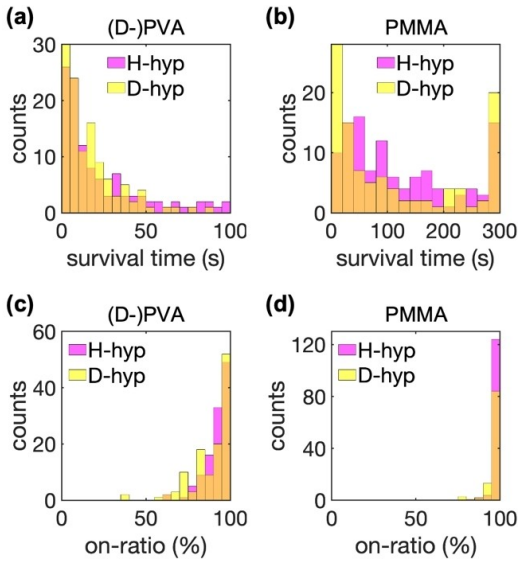

Figure 2. Statistics of single hypericin molecules' blinking behaviour. (a) and (b) shows the histogram of the survival times of single hypericin in different polymer matrices (n=115 for H-hypericin in PVA, n=121 for D-hypericin in D-PVA, n=131 for H-hypericin in PMMA, n=104 for D-hypericin in PMMA). Orange bars represent the overlap.

suppressed blinking dynamics, whereas the on-times of the molecules in PVA are competitive to their off-times with a significantly smaller k_{on}. Obviously, oxygen shortens the on-times of single molecules in PVA. This could be partially explained by the assumption that oxygen quenches the fluorescence by static quenching through an intermediate state, which then reversibly changes into another non- or less fluorescence state. Apart from the effect of oxygen on the blinking phenomena, we notice that deuterium plays an important role. Deuteration not only shortens the survival time, but also enhances the blinking on a much longer timescale. The fluctuations of the fluorescence intensity of D-hypericin seem to be much more pronounced than those H-hypericin. The origin of these observations will be discussed in the following.

Changes in the blinking dynamics are often accompanied by changes in the fluorescence lifetime. Therefore, we performed single-molecule TCSPC for (D-)hypericin in (D-)PVA and PMMA. As shown in Table 1, the average fluorescence lifetime τ_F is much longer in PMMA than in PVA, with no significant difference in standard deviation between H- and D-hypericin. A reduction of the fluorescence lifetime in PVA is observed, which

Table 1. Hydrogen/Deuterium isotope effects on fluorescence lifetimes τ_F of (H-/D−)hypericin (in ns). Empirical mean μ and standard deviation σ for the normal distribution and the median of fluorescence lifetimes of single hypericin molecules in different polymer matrices.

Matrix	Probe	μ [ns]	σ [ns]	Median [ns]
PVA	H-hypericin	3.7	0.8	3.7
D-PVA	D-hypericin	3.8	0.5	3.8
PMMA	H-hypericin	4.2	0.9	4.0
PMMA	D-hypericin	4.3	0.9	4.0

can be ascribed to H-bonding, as discussed in ensemble measurements.[29] Moreover, the fluorescence lifetime τ_F increases somewhat by deuteration in PVA (see Table 1).[29] The small deuterium isotope effect can be understood by analyzing τ_F, given by

$$1/\tau_F = k_r + k_{nr} \quad (1)$$

with k_r and k_{nr} as the radiative and non-radiative rates. Deuteration shows a negligible effect on k_r as the latter is related to the oscillator strength (*f*) and energy (E) of the emitting state (via the Strickler-Berg relation[30]), which are hardly changed upon deuteration (see SI for details). The component k_{nr} incorporates all other terms, which contribute to the overall decay rate, i.e. internal conversion (IC, with subsequent vibration relaxation, VR), intersystem crossing (ISC) towards the triplet manifold, and photochemical reactions like tautomerization, etc.[31] Deuteration has a pronounced effect on k_{IC}, but a negligible effect on k_{ISC}.[32] Therefore, the small isotope effect in hypericin, as also observed in related aromatic hydrocarbons,[33] suggests that $k_{ISC} \gg k_{IC}$, which agrees with the high triplet population of hypericin.[34] For IC, the rate k_{IC} can be estimated from Fermi's golden rule.[30b] Here, k_{IC} decreases with decreasing vibrational frequency (see SI for details), so that k_{IC} decreases upon deuteration because of smaller energy spacing between vibrational quanta (see SI for details).[35] This is in fact reflected in the much smaller total zero-point energy (0.37 eV) in the DFT calculations, while there is no significant difference in electronic and Gibbs free energies. This in all rationalizes the small, but notable increase of τ_F of D-hypericin in both polymer matrices in comparison with H-hypericin; see Figure 3. In any case, besides this *intra*molecular effect, we note a much

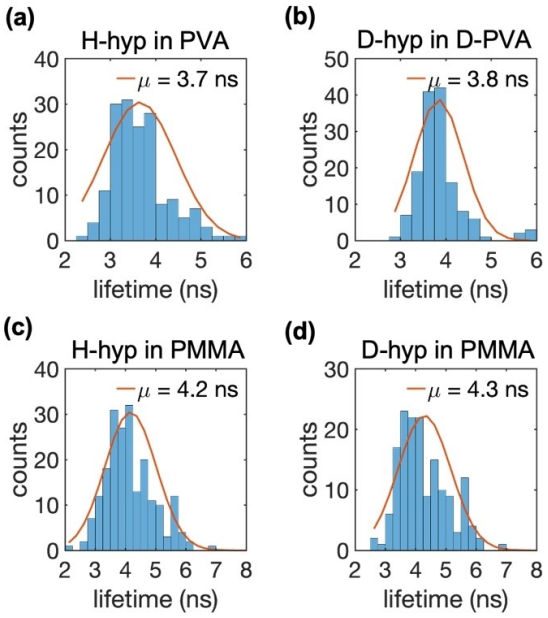

Figure 3. Histograms of derived fluorescence lifetime of single (H-/D−)hypericin molecules in (a) PVA (n=172), (b) D-PVA (n=147), (c) PMMA (n=175) and (d) PMMA (n=159). The red curves correspond to fitted Normal distributions associated with the mean values.

stronger effect for PVA than in PMMA; this points to a significant *inter*molecular contribution, which is evidently related to the possibility of H(D) bonding in the (D-)PVA matrix. This is expected to restrict the conformational freedom of hypericin, which in turn limits IC;[30b,36] this is indeed in line with the experimentally observed significant increase of τ_F and a narrower distribution for D-hypericin in D-PVA, as shown in Figure 3(b) and Table 1.

It is well established that tautomerization occurs via tunneling;[37] in organic molecules this is governed by the vibrational overlap. We thus expect that deuteration decreases the tautomerization rate, again due to the decreased energy spacing of the vibrational quanta; this was in fact observed in (ensemble) studies on various systems with largely different time constants.[38] In hypericin, tautomerization takes place in the second time range;[11] at a single molecule level, this can be monitored by fluorescence correlation spectroscopy (FCS),[39] which accumulates statistics from this complex many-event dynamics.[7b,12a,40] The intensity autocorrelation function (ACF), which reflects fluorescence intensity fluctuation dynamics,[41] can be calculated directly from the TCSPC data (with temporal resolution of 64 ps), as shown in Figure 4. The characteristic time of the fluctuations can be then extracted from a fluctuation time trace record with a model function. Here, we take into account two dynamic components, that is the triplet state lifetime (i.e. the short-time scale τ_1; i.e. in milliseconds) and the tautomerization process (the long-time scale τ_2; i.e. in seconds).

$$g^2(\tau) = G(\tau) - 1 \cong Ae^{-\left(\frac{t}{\tau_1}\right)^{\beta_1}} + Be^{-\left(\frac{t}{\tau_2}\right)^{\beta_2}} \quad (2)$$

It is noted that, if the multiple events by accident occur within the same temporal integration time, the evaluated lifetime gives the information on the average value of all the processes involved.

In the following, we will discuss one representative result of a FCS analysis, which was fitted with eq. (2), giving $\tau_1 = 7.8$ ms and $\tau_2 = 12.0$ s. We note strong deviations at shorter time lag, ($> 10^{-1}$ ms), ascribed to triplet blinking, while the minor deviations at medium time lag (10^{-1} ~10^2 ms) point to a more complex photophysics occurring from the triplet state, which may reflect, for instance, reorganization of the environment; finally, at long time lag ($> 10^2$ ms), the residuals converge to zero. Additional information can be obtained from the stretch parameters β ($\beta_1 = 0.62$, $\beta_2 = 0.32$); the latter allow to draw conclusions on how many processes are occurring in the corresponding time window. The first parameter $\beta_1 = 0.62$ is indicative of a large portion of short-time dynamics (τ_1). The second parameter shows only a minor contribution ($\beta_2 = 0.32$), reflecting the dominance of the short-time scale (triplet blinking) in the temporal emission behavior.

The histograms in Figure 5 show the distribution of the $< \tau_1 >$ and $< \tau_2 >$ for single (D-)hypericin in (D-)PVA and PMMA. The short-time fluctuation (~ ms) of hypericin in PVA shows a normal distribution with $< \tau_1 > = 6.7$ ms, whereas the D-hypericin follows a Poisson distribution and yields an average lifetime of 5.0 ms. Such inverse deuterium isotope effect in residing time τ_1 is not expected, if deactivation by ISC to the ground state (GS) is concerned;[32] this implies the involvement of other photophysical and/or -chemical processes from the triplet state, which are affected by deuteration, governed by τ_2, exhibits a significant deuterium isotope effect with an increase of the residing time $< \tau_2 >$, from 2.9 to 3.9 s, when going from H- to D-hypericin in (D-)PVA. As discussed before, this agrees with the expectation from the consideration on tunneling of a proton.

Changing the matrix to PMMA, the on-off triplet blinking behavior $< \tau_1 >$ is largely suppressed, see Figure 2 (d);this may be due to the fact that the ISC rate in PMMA is much lower than in PVA, thus only a small number of hypericin molecules proceeds to the triplet manifold. For the long-time fluctuations, in comparison with PVA, tautomerization in PMMA appears to be less favored, consistent with the observations in the short-time scale (the average lifetime $< \tau_2 > = 1.5$ s for H- and $< \tau_2 > = 2.3$ s for D-hypericin in PMMA). We anyway note that, under certain circumstances, there is no apparent short/long timescale dynamics; this leads to a single exponential character with one component $\tau_{1/2} = \infty$. To indicate the probability of occurrence, we set all infinite fitting results to 20 ms and 40 s, respectively.

In order to rationalize the specific impact of the *inter*molecular interaction between (D-)hypericin and the polymer matrix, we conducted (TD)DFT calculations of the isolated hypericin molecule in methanol (using the implicit PCM model) and the explicit cluster model (hypericin embedded in the realistic polymer environment). The equilibrium geometries at the ground state (GS) and the transition state (TS) were obtained to investigate the stereochemistry and contributing geometrical & electronic factors (for further details see SI). Following our previous results on the tautomerization process,[11–12] we focus on three dominating dihedral angles as indicated in Figure 1(d): the methyl (θ_{Me}) and hydroxyl (θ_{OH})

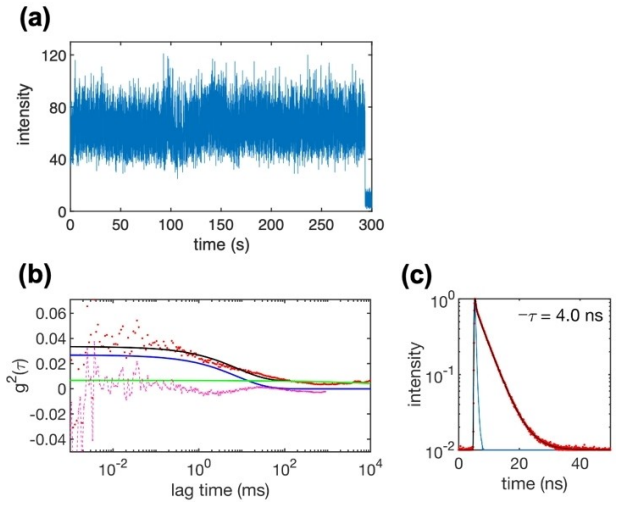

Figure 4. (a) The intensity time trace of a single hypericin molecule in PMMA and the corresponding (b) intensity autocorrelation functions $g^2(\tau)$ (the black curve) as well as (c) the fluorescence lifetime. The molecule shows a short-time blinking ($\tau_1 = 7.8$ ms, the blue curve) and a long-time fluctuation ($\tau_2 = 12.0$ s, the green curve) with the fluorescence lifetime $\tau_F = 4.0$ ns. A residual analysis is indicated in magenta dashed line.

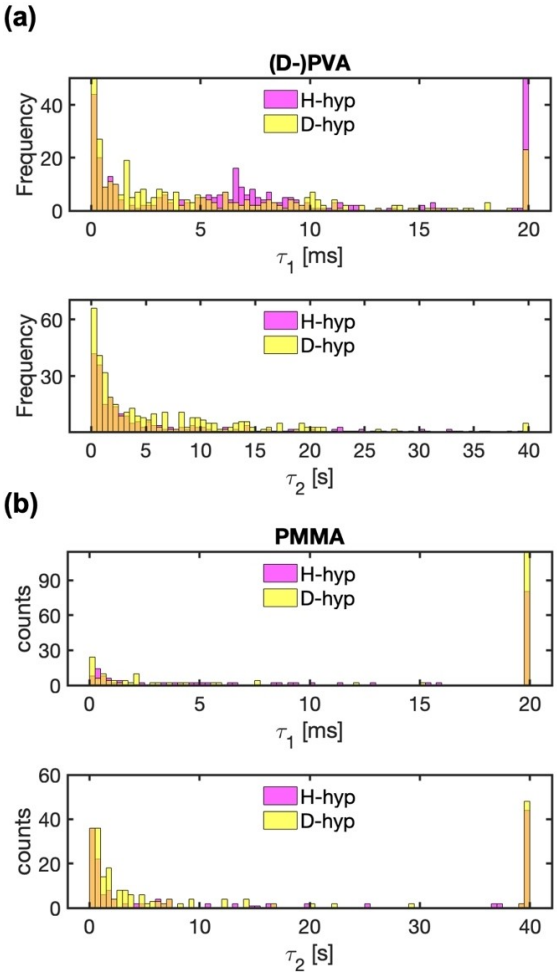

Figure 5. Histograms of the dynamic parameters for single hypericin molecules in (D-)PVA (n=357, n=423 for H- and D-hypericin) and in PMMA (n=186, n=246 for H- and D-hypericin). $<\tau_1>$ refers to the fast fluctuation dynamics, i.e. a triplet quenching process, while $<\tau_2>$ refers to the slow fluctuation dynamics, i.e. the tautomerization process. Orange bars represent the overlap.

groups at the *bay* region, which are responsible for the distortion of the aromatic parent backbone; and the hydroxyl group (θ_{OH}) at the *peri* region, where the proton transfer occurs at the TS. In a previous study, we showed a detailed picture of tautomerization pathways for the isolated molecule;[11] i.e. without considering environmental effects. In a simple way, the latter can be treated in an implicit manner, for instance by PCM; this model however only considers polarizability effects. Therefore, it is essential to apply an explicit model with a realistic electronic environment. In fact, it can be seen in Table 2 that the hypericin geometry in PMMA is very similar to that in methanol, suggesting that PMMA itself serves as an 'innocent' solvent. In stark contrast, according to the calculations, hypericin is more distorted in PVA, which can be attributed to efficient *inter*molecular hydrogen bonding with the host polymer. In any case, the higher free volume in PVA due to the high water content may contribute to the experimental observations, an effect which was not considered in the calculations. From the energy point of view, the activation

Table 2. Descriptions of the calculated structure at the ground state (GS) and the transition state (TS) for single hypericin molecule in MeOH (PCM), and the cluster model using D3-B3LYP with the standard basis set 6–31G(d).

Dihedral angle (°)	MeOH (PCM)		PVA		PMMA	
	GS	TS	GS	TS	GS	TS
θ_{Me} (bay)	33	34	40	45	36	37
θ_{OH} (bay)	27	27	24	25	29	30
θ_{OH} (TS)	1	102	8	120	3	113

barrier for tautomerization is 0.18 eV higher in PMMA than in PVA, which indicates that tautomerization is more energetically favored in PVA in agreement with the experimental observations.Conclusions

In conclusion, we have investigated the deuterium isotope effect on the photophysics and photochemistry of hypericin at the single-molecule level in different polymer matrices by a combined spectroscopic and computational approach. Two different polymers (PVA, PMMA) were used to investigate the influence of the local chemical environment. The hydroxyl group in PVA favors to form an H(D) bond with hypericin, giving rise to significant *inter*molecular solute-solvent interactions. In contrast, PMMA can be considered as an 'innocent' polymer host, as it does not provide such functionalities but benefits from photo-stabilization (a longer survival time) due to low oxygen exposure. Because of the high water content in PVA, this matrix has proven to be a good candidate to study the deuterium isotope effect on hypericin, and its decay mechanism of excited states. Deuterium increases the fluorescence lifetime, however the effect is shown to be small; this is due to the high triplet generation in hypericin, so that internal conversion, which is most affected by deuteration, is a minor pathway. Deuteration further decreases nonradiative decay of the triplet state as well as the tautomerization rate. All this can be rationalized by the decrease of energy spacing of vibrational quanta upon deuteration. Finally, in combination with the experimental observations, (TD)DFT calculations provide in-depth understanding of specific nano-environmental interactions between hypericin and the polymer matrix at the electronic level. In all, this work may pave the way to monitor and even control the photophysics and photochemistry of probe molecules at a single-molecule level.

Acknowledgements

The authors acknowledge support by the state of Baden-Württemberg through bwHPC and the German Research Foundation (DFG) through grants ME 1600_13-3 and INST 40/575-1 FUGG (JUSTUS 2 cluster). J.G. acknowledges funding from Spanish Ministerio de Ciencia e Innovación (MICIN-FEDER) project PID2022-138222NB–C21). The work in Madrid was additionally supported by the Severo Ochoa program for Centers of Excellence in R&D of the MICIN (CEX2020-001039-S)

and by the Campus of International Excellence (CEI) UAM+CSIC. L.W. thanks Dr. Juan Carlos Roldao and Jonas Hiller for the fruitful discussion. We thank Pablo Gierschner Milián (Valencia) for assistance in the artwork. Open Access funding enabled and organized by Projekt DEAL.

Conflict of Interests

The authors declare no conflict of interest.

Data Availability Statement

The data that support the findings of this study are available in the supplementary material of this article.

Keywords: single molecule spectroscopy · tautomerization · deuteration · nano-environmental effect · density functional theory

[1] M. F. Serag, M. Abadi, S. Habuchi, *Nat. Commun.* **2014**, *5*, 5123.
[2] M. Kinjo, R. Rigler, *Nucleic Acids Res.* **1995**, *23*, 1795–1799.
[3] a) B. Rauer, E. Neumann, J. Widengren, R. Rigler, *Biophys. Chem.* **1996**, *58*, 3–12; b) B. Niewidok, M. Igaev, A. Pereira da Graca, A. Strassner, C. Lenzen, C. P. Richter, J. Piehler, R. Kurre, R. Brandt, *J. Cell Biol.* **2018**, *217*, 1303–1318.
[4] a) D. Brinks, F. D. Stefani, F. Kulzer, R. Hildner, T. H. Taminiau, Y. Avlasevich, K. Müllen, N. F. van Hulst, *Nature* **2010**, *465*, 905–908; b) Y. Goto, S. Omagari, R. Sato, T. Yamakado, R. Achiwa, N. Dey, K. Suga, M. Vacha, S. Saito, *J. Am. Chem. Soc.* **2021**; c) A. M. Chizhik, R. Jager, A. I. Chizhik, S. Bar, H. G. Mack, M. Sackrow, C. Stanciu, A. Lyubimtsev, M. Hanack, A. J. Meixner, *Phys. Chem. Chem. Phys.* **2011**, *13*, 1722–1733.
[5] S. Skandary, A. Konrad, M. Hussels, A. J. Meixner, M. Brecht, *J. Phys. Chem. B* **2015**, *119*, 13888–13896.
[6] Z. Liu, L. D. Lavis, E. Betzig, *Mol. Cell* **2015**, *58*, 644–659.
[7] a) W. E. Moerner, Y. Shechtman, Q. Wang, *Faraday Discuss.* **2015**, *184*, 9–36; b) S. Adhikari, M. Orrit, *J. Chem. Phys.* **2022**, *156*, 160903; c) F. Persson, I. Barkefors, J. Elf, *Curr. Opin. Biotechnol.* **2013**, *24*, 737–744; d) W. E. Moerner, *Angew. Chem. Int. Ed. Engl.* **2015**, *54*, 8067–8093; e) M. Orrit, T. Ha, V. Sandoghdar, *Chem. Soc. Rev.* **2014**, *43*, 973–976; f) A. M. Kern, D. Zhang, M. Brecht, A. I. Chizhik, A. V. Failla, F. Wackenhut, A. J. Meixner, *Chem. Soc. Rev.* **2014**, *43*, 1263–1286.
[8] a) M. J. Fehr, M. McCloskey, J. W. Petrich, *J. Am. Chem. Soc.* **1995**, *117*, 1833–1836; b) D. S. English, K. Das, K. D. Ashby, J. Park, J. W. Petrich, E. W. Castner, *J. Am. Chem. Soc.* **1997**, *119*, 11585–11590.
[9] a) A. Kubin, F. Wierrani, U. Burner, G. Alth, W. Grunberger, *Curr. Pharm. Des.* **2005**, *11*, 233–253; b) P. Agostinis, A. Vantieghem, W. Merlevede, P. A. M. de Witte, *Int. J. Biochem. Cell Biol.* **2002**, *34*, 221–241; c) T. A. Theodossiou, J. S. Hothersall, P. A. De Witte, A. Pantos, P. Agostinis, *Mol. Pharm.* **2009**, *6*, 1775–1789.
[10] a) H. Falk, K. Wolkenstein, *Prog. Chem. Org. Nat. Prod.* **2017**, *104*, 1–126; b) H. Falk, *Angew. Chem. Int. Ed. Engl.* **1999**, *38*, 3116–3136; c) C. Etzlstorfer, H. Falk, *Monatsh. Chem.* **1998**, *129*, 855–863; d) R. Altmann, H. Falk, *Monatsh. Chem.* **1997**, *128*, 571–583; e) H. Falk, J. Meyer, *Monatsh. Chem.* **1994**, *125*, 753–762; f) C. Etzlstorfer, H. Falk, N. Müller, W. Schmitzberger, U. G. Wagner, *Monatsh. Chem.* **1993**, *124*, 751–761; g) C. Etzlstorfer, H. Falk, M. Oberreiter, *Monatsh. Chem.* **1993**, *124*, 923–929; h) A. Angerhofer, H. Falk, J. Meyer, G. Schoppel, *J. Photochem. Photobiol. B* **1993**, *20*, 133–137.
[11] a) Q. Liu, F. Wackenhut, L. Wang, O. Hauler, J. C. Roldao, P. M. Adam, M. Brecht, J. Gierschner, A. J. Meixner, *J. Phys. Chem. Lett.* **2021**, *12*, 1025–1031; b) Q. Liu, L. Wang, J. C. Roldao, P. M. Adam, M. Brecht, J. Gierschner, F. Wackenhut, A. J. Meixner, *Adv. Photonics Res.* **2021**, *2*, 2000170.
[12] a) Q. Liu, L. Wang, J. C. Roldao, P.-M. Adam, M. Brecht, J. Gierschner, F. Wackenhut, A. J. Meixner, *Adv. Photonics Res.* **2021**, *2*; b) L. Wang, Q. Liu, F. Wackenhut, M. Brecht, P. M. Adam, J. Gierschner, A. J. Meixner, *J. Chem. Phys.* **2022**, *156*, 014203.
[13] a) C. A. Hutchison Jr, B. W. Mangum, *J. Chem. Phys.* **1960**, *32*; b) M. M. Martin, L. Lindqvist, *Chem. Phys. Lett.* **1973**, *22*, 309–312; c) M. Kusinski, J. Nagesh, M. Gladkikh, A. F. Izmaylov, R. A. Jockusch, *Phys. Chem. Chem. Phys.* **2019**, *21*, 5759–5770.
[14] J. L. Wynn, T. M. Cotton, *J. Phys. Chem.* **1995**, *99*, 4317–4323.
[15] a) R. Verberk, M. Orrit, *J. Chem. Phys.* **2003**, *119*, 2214–2222; b) R. Verberk, A. M. van Oijen, M. Orrit, *Phys. Rev. B* **2002**, *66*, 233202.
[16] W. Becker, *Advanced time-correlated single photon counting applications*, *Vol. 111*, Springer, **2015**.
[17] ALLRESIST, Positive PMMA E-Beam Resists AR–P 630 – 670 series, can be found under https://www.allresist.com/wp-content/uploads/sites/2/2021/02/Allresist_Product-information-E-Beamresist-AR–P-630–670-English-web.pdf (accessed 2024–03-13).
[18] M. J. Frisch, G. W. Trucks, H. B. Schlegel, G. E. Scuseria, M. A. Robb, J. R. Cheeseman, G. Scalmani, V. Barone, G. A. Petersson, H. Nakatsuji, X. Li, M. Caricato, A. V. Marenich, J. Bloino, B. G. Janesko, R. Gomperts, B. Mennucci, H. P. Hratchian, J. V. Ortiz, A. F. Izmaylov, J. L. Sonnenberg, Williams, F. Ding, F. Lipparini, F. Egidi, J. Goings, B. Peng, A. Petrone, T. Henderson, D. Ranasinghe, V. G. Zakrzewski, J. Gao, N. Rega, G. Zheng, W. Liang, M. Hada, M. Ehara, K. Toyota, R. Fukuda, J. Hasegawa, M. Ishida, T. Nakajima, Y. Honda, O. Kitao, H. Nakai, T. Vreven, K. Throssell, J. A. Montgomery Jr., J. E. Peralta, F. Ogliaro, M. J. Bearpark, J. J. Heyd, E. N. Brothers, K. N. Kudin, V. N. Staroverov, T. A. Keith, R. Kobayashi, J. Normand, K. Raghavachari, A. P. Rendell, J. C. Burant, S. S. Iyengar, J. Tomasi, M. Cossi, J. M. Millam, M. Klene, C. Adamo, R. Cammi, J. W. Ochterski, R. L. Martin, K. Morokuma, O. Farkas, J. B. Foresman, D. J. Fox, Wallingford, CT, **2016**.
[19] L. Martinez, R. Andrade, E. G. Birgin, J. M. Martinez, *J. Comput. Chem.* **2009**, *30*, 2157–2164.
[20] M. J. Abraham, T. Murtola, R. Schulz, S. Páll, J. C. Smith, B. Hess, E. Lindahl, *SoftwareX* **2015**, *1–2*, 19–25.
[21] I. Tuñón, I. H. Williams, **2019**, pp. 29–68.
[22] Q. Liu, F. Wackenhut, O. Hauler, M. Scholz, S. Zur Oven-Krockhaus, R. Ritz, P. M. Adam, M. Brecht, A. J. Meixner, *J. Phys. Chem. A* **2020**, *124*, 2497–2504.
[23] J. J. Macklin, J. K. Trautman, T. D. Harris, L. E. Brus, *Science* **1996**, *272*, 255–258.
[24] a) M. Joesten, L. Schaad, M. Tamres, American Institute of Physics, **1975**; b) R. P. Bell, *The proton in chemistry*, Springer Science & Business Media, **2013**; c) S. Scheiner, M. Čuma, *J. Am. Chem. Soc.* **1996**, *118*, 1511–1521.
[25] W.-H. Yang, V. F. Smolen, N. A. Peppas, *J. Membr. Sci.* **1981**, *9*, 53–67.
[26] C. Book, Product Description: 9002–89-5 (Poly(vinyl alcohol)) can be found under https://www.chemicalbook.com/ChemicalProductProperty_US_CB7264573.aspx (accessed 2024–03-13).
[27] a) A. Renn, S. E. Bucher, A. J. Meixner, E. C. Meister, U. P. Wild, *J. Lumin.* **1988**, *39*, 181–187; b) A. J. Meixner, A. Renn, U. P. Wild, *Chem. Phys. Lett.* **1992**, *190*, 75–82; c) A. J. Meixner, A. Renn, S. E. Bucher, U. P. Wild, *J. Phys. Chem.* **2002**, *90*, 6777–6785.
[28] a) O. Panzer, W. Göhde, U. C. Fischer, H. Fuchs, K. Müllen, *Adv. Mater.* **1998**, *10*, 1469–1472; b) R. Zondervan, F. Kulzer, S. B. Orlinskii, M. Orrit, *J. Phys. Chem. A* **2003**, *107*, 6770–6776; c) F. Stracke, C. Blum, S. Becker, K. Müllen, A. J. Meixner, *ChemPhysChem* **2005**, *6*, 1242–1246.
[29] T. Yamazaki, N. Ohta, I. Yamazaki, P. S. Song, *J. Phys. Chem.* **1993**, *97*, 7870–7875.
[30] a) S. J. Strickler, R. A. Berg, *J. Chem. Phys.* **1962**, *37*, 814–822; b) J. Gierschner, J. Shi, B. Milián-Medina, D. Roca-Sanjuán, S. Varghese, S. Park, *Adv. Opt. Mater.* **2021**, *9*.
[31] W. Browne, *Coord. Chem. Rev.* **2001**, *219–221*, 761–787.
[32] N. J. Turro, V. Ramamurthy, J. C. Scaiano, *Modern molecular photochemistry of organic molecules*, *Vol. 188*, University Science Books Sausalito, CA, **2010**.
[33] J. D. Laposa, E. C. Lim, R. E. Kellogg, *J. Chem. Phys.* **1965**, *42*, 3025–3026.
[34] P. Jardon, N. Lazorchak, R. Gautron, *Journal de chimie physique* **1986**, *83*, 311–315.
[35] J. M. Martin Klessinger, *Excited States and Photo-Chemistry of Organic Molecules*, *Revised and Improved English-Language Edition*, Wiley, **1995**.
[36] J. Shi, L. E. Aguilar Suarez, S.-J. Yoon, S. Varghese, C. Serpa, S. Y. Park, L. Lüer, D. Roca-Sanjuán, B. Milián-Medina, J. Gierschner, *J. Phys. Chem. C* **2017**, *121*, 23166–23183.
[37] a) J. Marañon, O. M. Sorarrain, *Z. Naturforsch.* **1979**, *34*, 315–319; b) T. J. Butenhoff, C. B. Moore, *J. Am. Chem. Soc.* **2002**, *110*, 8336–8341.

[38] a) A. Douhal, S. K. Kim, A. H. Zewail, *Nature* **1995**, *378*, 260–263; b) J. Braun, M. Koecher, M. Schlabach, B. Wehrle, H.-H. Limbach, E. Vogel, *J. Am. Chem. Soc.* **1994**, *116*, 6593–6604.
[39] a) M. A. Digman, E. Gratton, *Annu. Rev. Phys. Chem.* **2011**, *62*, 645–668; b) E. Haustein, P. Schwille, *Annu. Rev. Biophys. Biomol. Struct.* **2007**, *36*, 151–169.
[40] a) H. Yuan, T. Xia, B. Schuler, M. Orrit, *Phys. Chem. Chem. Phys.* **2011**, *13*, 1762–1769; b) H. Yuan, A. Gaiduk, J. R. Siekierzycka, S. Fujiyoshi, M. Matsushita, D. Nettels, B. Schuler, C. A. Seidel, M. Orrit, *Phys. Chem. Chem. Phys.* **2015**, *17*, 6532–6544.
[41] S. R. Aragón, R. Pecora, *J. Chem. Phys.* **1976**, *64*, 1791–1803.

Manuscript received: April 1, 2024
Revised manuscript received: May 20, 2024
Accepted manuscript online: June 5, 2024
Version of record online: ■■, ■■

RESEARCH ARTICLE

The detailed photophysics and -chemistry of organic chromophores may depend significantly on the nano-environment. However, in ensemble measurements only an average behavior can be observed in ensemble measurements. Therefore, we investigate herein the deuterium (D) isotope effect on hypericin tautomerization in the ambient at the single-molecule level in different polymer matrices by a combined spectroscopic and computational approach.

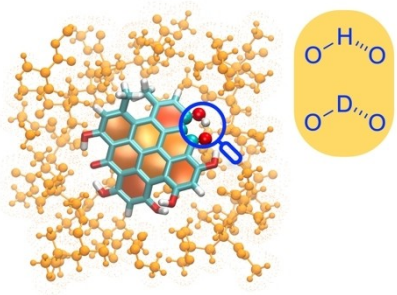

L. Wang, Dr. Q. Liu, A. Buchwald, Dr. F. Wackenhut, Dr. M. Brecht, Dr. J. Gierschner, Prof. Dr. A. J. Meixner**

1 – 9

Deuterium Isotope Effect in Single Molecule Photophysics and Photochemistry of Hypericin